Traffic within the Cytochrome b_6f Lipoprotein Complex: Gating of the Quinone Portal

S. Saif Hasan,[1] Elizabeth A. Proctor,[2] Eiki Yamashita,[3] Nikolay V. Dokholyan[4] and William A. Cramer[1¶]

SUPPLEMENTARY INFORMATION

SI Table T1A. Crystallographic data summary. Average strength of reflection, i.e., $\langle I \rangle / \langle \sigma_I \rangle$, is shown as a function of resolution. CC*, the correlation coefficient for data-merging, is defined in reference (38) in the main text.

Resolution (Å)	$\langle I \rangle$	$\langle \sigma_I \rangle$	$\langle I \rangle / \langle \sigma_I \rangle$	R_{pim}	CC*	Completeness (%)
50.00-8.13	474	11.5	41.2	0.012	1	97.8
8.13-6.46	156.9	5	31.4	0.018	1	100.0
6.46-5.64	79.9	3.1	25.8	0.028	0.999	100.0
5.64-5.13	87.7	3.5	25.1	0.028	0.999	100.0
5.13-4.76	102.6	4.1	25	0.028	0.999	100.0
4.76-4.48	96.9	4	24.2	0.028	0.999	100.0
4.48-4.26	78.6	3.7	21.2	0.034	0.999	100.0
4.26-4.07	59.6	3.4	17.5	0.042	0.998	100.0
4.07-3.91	44.5	3	14.8	0.054	0.998	100.0
3.91-3.78	36.2	2.9	12.5	0.066	0.996	100.0
3.78-3.66	24.3	3	8.1	0.099	0.991	100.0
3.66-3.56	20.3	3.1	6.6	0.122	0.987	99.9
3.56-3.46	15.8	3.2	4.9	0.149	0.981	99.9
3.46-3.38	11.7	3.4	3.4	0.194	0.969	99.7
3.38-3.30	9.0	3.8	2.4	0.246	0.939	99.1
3.30-3.23	7.2	4.4	1.6	0.288	0.902	94.9
3.23-3.17	6.1	5	1.2	0.292	0.92	82.6
3.17-3.11	5.2	5.5	0.9	0.408	0.843	65.6
3.11-3.05	3.8	5.4	0.7	0.486	0.803	47.5
3.05-3.00	3.3	5.8	0.6	0.647	0.807	38.0

SI Table T1B. Crystallographic data summary. Distribution of reflections is shown as a function of resolution.

Resolution (Å)	**Total**	**(I/<σ_I>) <0**	**(I/<σ_I>) <1**	**(I/<σ_I>) <2**	**(I/<σ_I>) <3**	**(I/<σ_I>) <5**	**(I/<σ_I>) <10**	**(I/<σ_I>) <20**	**(I/<σ_I>) >20**
50.00-8.13	3018	19	38	50	68	89	149	328	2690
8.13-6.46	2872	28	60	95	131	183	340	858	2014
6.46-5.64	2823	48	107	156	207	306	567	1255	1568
5.64-5.13	2782	49	98	136	182	277	530	1239	1543
5.13-4.76	2779	44	79	131	183	286	518	1188	1591
4.76-4.48	2771	70	116	188	241	362	673	1358	1413
4.48-4.26	2748	70	123	220	298	452	837	1573	1175
4.26-4.07	2729	76	185	291	409	602	1045	1848	881
4.07-3.91	2754	106	242	376	518	785	1319	2053	701
3.91-3.78	2721	134	287	481	652	957	1505	2136	585
3.78-3.66	2729	195	410	666	878	1262	1861	2437	292
3.66-3.56	2711	218	487	772	1033	1440	2050	2523	188
3.56-3.46	2693	262	586	984	1264	1716	2269	2581	112
3.46-3.38	2723	372	796	1270	1639	2057	2465	2656	67
3.38-3.30	2677	440	966	1466	1799	2196	2526	2649	28
3.30-3.23	2567	524	1129	1654	1981	2271	2476	2549	18
3.23-3.17	2238	570	1147	1594	1840	2013	2175	2226	12
3.17-3.11	1763	470	972	1337	1522	1663	1742	1761	2
3.11-3.05	1283	375	782	1043	1144	1229	1269	1282	1
3.05-3.00	1016	342	656	870	945	987	1012	1016	0

SI Table T1C. Crystallographic data summary. Distribution of reflection strength, in percentage, is shown as a function of resolution.

Resolution (Å)	$(I/<\sigma_I>)$ <0	0≤ $(I/<\sigma_I>)$ <1	1≤ $(I/<\sigma_I>)$ <2	2≤ $(I/<\sigma_I>)$ <3	3≤ $(I/<\sigma_I>)$ <5	5≤ $(I/<\sigma_I>)$ <10	10≤ $(I/<\sigma_I>)$ <20	$(I/<\sigma_I>)$ >20
50.00-8.13	0.6	0.6	0.4	0.6	0.7	2	5.9	89.1
8.13-6.46	1.0	1.1	1.2	1.3	1.8	5.5	18.0	70.1
6.46-5.64	1.7	2.1	1.7	1.8	3.5	9.2	24.4	55.5
5.64-5.13	1.8	1.8	1.4	1.7	3.4	9.1	25.5	55.5
5.13-4.76	1.6	1.3	1.9	1.9	3.7	8.3	24.1	57.3
4.76-4.48	2.5	1.7	2.6	1.9	4.4	11.2	24.7	51.0
4.48-4.26	2.5	1.9	3.5	2.8	5.6	14	26.8	42.8
4.26-4.07	2.8	4	3.9	4.3	7.1	16.2	29.4	32.3
4.07-3.91	3.8	4.9	4.9	5.2	9.7	19.4	26.7	25.5
3.91-3.78	4.9	5.6	7.1	6.3	11.2	20.1	23.2	21.5
3.78-3.66	7.1	7.9	9.4	7.8	14.1	21.9	21.1	10.7
3.66-3.56	8.0	9.9	10.5	9.6	15.0	22.5	17.4	6.9
3.56-3.46	9.7	12	14.8	10.4	16.8	20.5	11.6	4.2
3.46-3.38	13.7	15.6	17.4	13.6	15.4	15.0	7.0	2.5
3.38-3.30	16.4	19.6	18.7	12.4	14.8	12.3	4.6	1.0
3.30-3.23	20.4	23.6	20.5	12.7	11.3	8.0	2.8	0.7
3.23-3.17	25.5	25.8	20.0	11.0	7.7	7.2	2.3	0.5
3.17-3.11	26.7	28.5	20.7	10.5	8.0	4.5	1.1	0.1
3.11-3.05	29.2	31.7	20.3	7.9	6.6	3.1	1	0.1
3.05-3.00	33.7	30.9	21.1	7.4	4.1	2.5	0.4	0.0

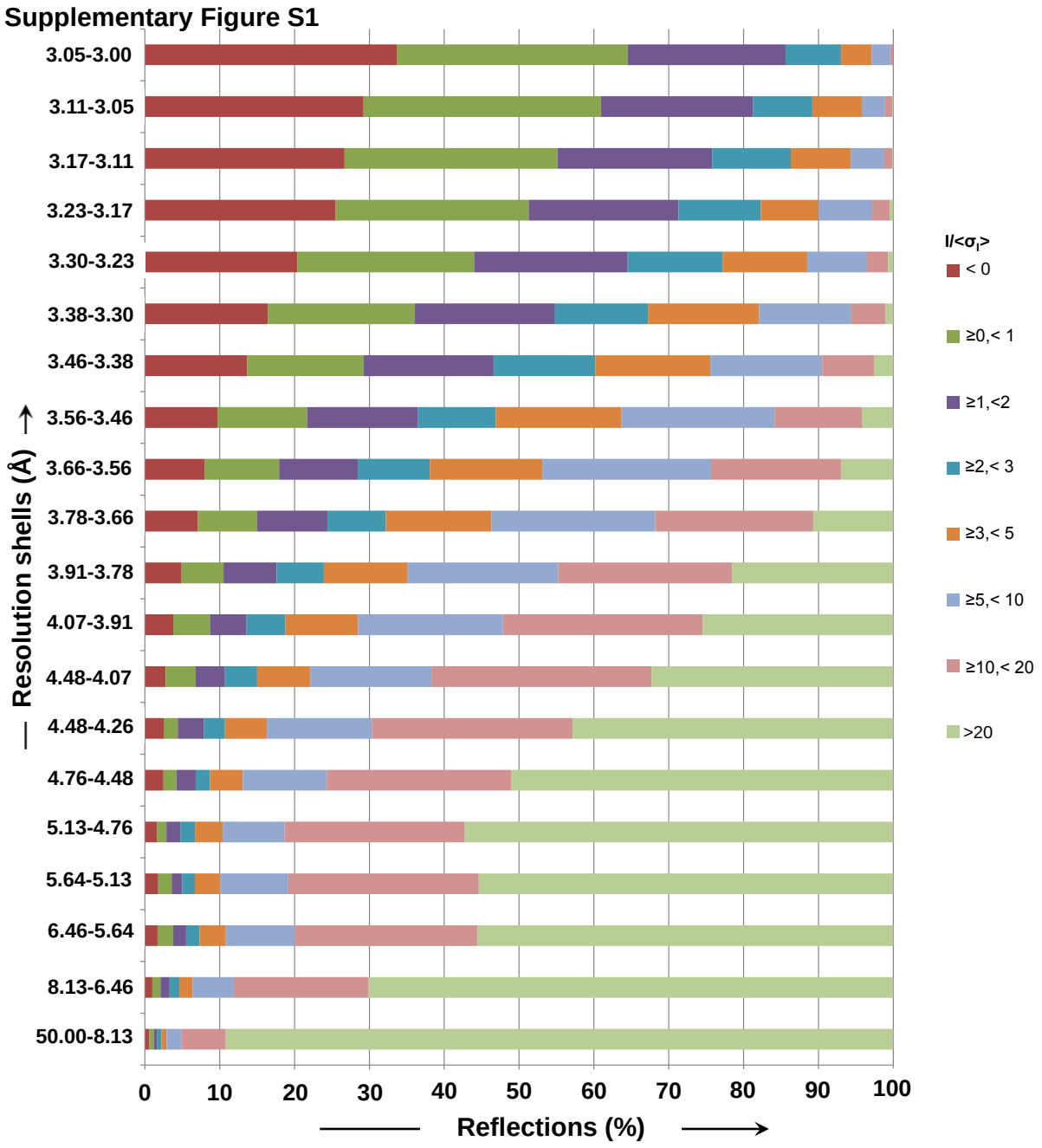

Figure S1. *Percentage of strong reflections decreases rapidly with increasing resolution.* The stronger reflections provide a measure of the average reflection strength, *i.e.*, $\langle I \rangle / \langle \sigma_I \rangle$, value per shell (see **Supplementary Table T1B,C** for details). Hence, the rapid decrease in average signal strength, *i.e.*, $\langle I \rangle / \langle \sigma_I \rangle$, is due to the decreasing contribution of the stronger reflections to the over-all average intensity. The reflection categories are color coded according to $I/\langle \sigma_I \rangle$.

Supplementary Figure S2

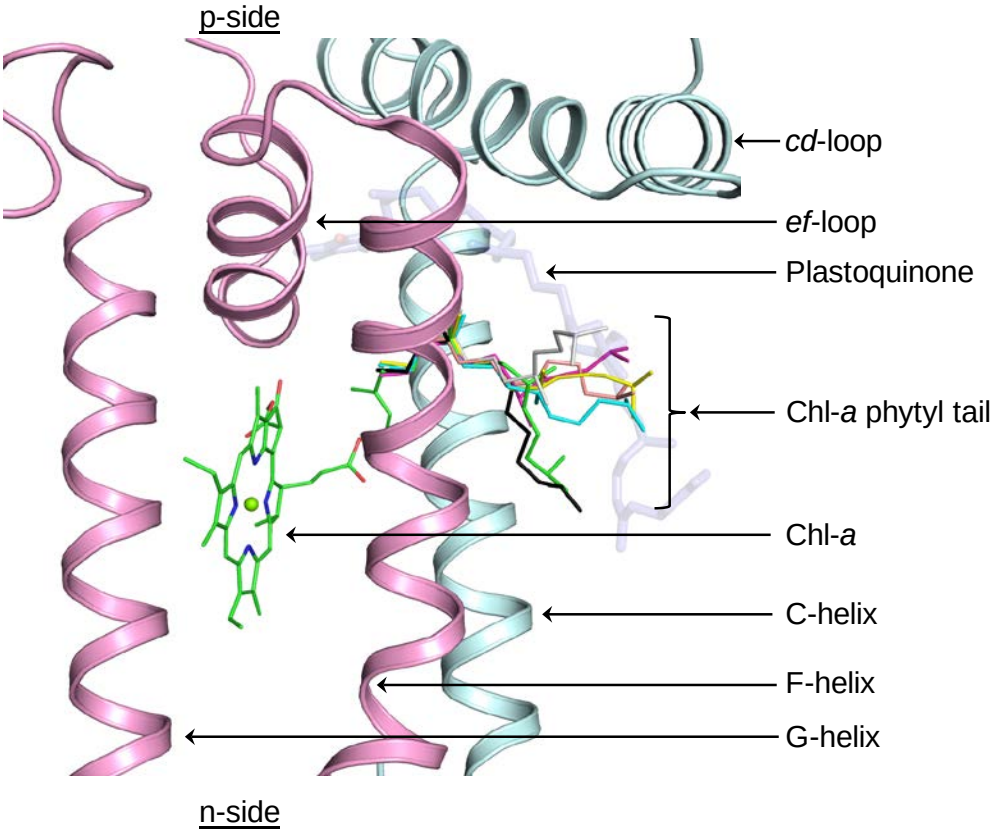

Figure S2. *Mobile phytyl-tail of Chl during DMD simulation.* The Chl phytyl-tail (shown as thin sticks) undergoes extensive motion during the course of the simulation. Color code- green, 0.0 ns; black, 2.5 ns; cyan, 5.0 ns; pink, 7.5 ns, yellow, 10.0 ns, light brown 12.5 ns; gray, 15 ns. For reference, plastoquinone bound in the Q_p-site is shown as semi-transparent thick sticks, and the protein environment is shown as ribbons (cyt b_6, cyan; subIV, pink).